Strain-displacement relations and strain engineering in 2d materials

Daniel Midtvedt,[1] Caio H. Lewenkopf,[2] and Alexander Croy[1,*]

[1] *Max-Planck-Institute for the Physics of Complex Systems, Dresden, Germany*
[2] *Universidade Federal Fluminense, Niterói, Brazil*

We investigate the electromechanical coupling in 2d materials. For non-Bravais lattices, we find important corrections to the standard macroscopic strain - microscopic atomic-displacement theory. We put forward a general and systematic approach to calculate strain-displacement relations for several classes of 2d materials. We apply our findings to graphene as a study case, by combining a tight binding and a valence force-field model to calculate electronic and mechanical properties of graphene nanoribbons under strain. The results show good agreement with the predictions of the Dirac equation coupled to continuum mechanics. For this long wave-limit effective theory, we find that the strain-displacement relations lead to a renormalization correction to the strain-induced pseudo-magnetic fields. Implications for nanomechanical properties and electromechanical coupling in 2d materials are discussed.

arXiv:1509.02365v1 [cond-mat.mes-hall] 8 Sep 2015

I. INTRODUCTION

Linear continuum elasticity provides a valuable basis for the investigation of the mechanical properties of atomic monolayer materials[1, 2]. Elastic theory is also a key element for understanding the relation between the material deformations and the corresponding modifications of its electronic structure[2–4]. Roughly speaking, strain changes the interatomic distances, thereby modulating the overlap of electronic orbitals of neighboring atoms and modifying the electronic properties of the material. To model and engineer this electromechanical coupling it is necessary to correctly relate experimentally controllable macroscopic deformations, parametrized by the strain tensor $\mathfrak{u}$, to microscopic atomic displacements.

We find that for materials with a crystal structure with a basis there is an important correction to the standard strain-displacement relations. We show that by applying strain to a 2d monolayer material, the nearest-neighbor vectors connecting the atoms transform as $\mathbf{r}_{ij} \to (\mathfrak{I}_3 + \mathfrak{u}) \cdot \mathbf{r}_{ij} + \boldsymbol{\Delta}$, where $\mathfrak{I}_n$ is the $n \times n$ identity matrix and $\boldsymbol{\Delta}$ is a vector that depends on the material deformation energy.

In this Letter we provide a transparent and systematic approach to calculate the strain-deformation relations for any kind of 2d material, provided that the deformation energy can be parametrized in terms of the bond vectors. We show the significance of our findings by contrasting the elastic bulk properties of graphene and black phosphorous calculated with and without the proposed corrections.

We study the effect of the strain-displacement corrections on electronic degrees of freedom in two applications. In the first one we incorporate the modified strain-displacement relations in the extensively used $\mathbf{k} \cdot \mathbf{p}$ theory for graphene, where strain can be represented by an effective gauge field[5–7]. We show that a correct assessment of $\boldsymbol{\Delta}$ renormalizes the strength of the gauge vector-potential by a factor 3/5, which means a factor $(3/5)^2$ for scattering rates relevant to transport properties [8, 9]. A similar correction has previously been identified in the study of the elastic properties of carbon nanotubes, where the strain-deformation relations were inferred from the analysis of the acoustic phonon modes[5, 10]. In the second application we study the effect of our findings on the gap engineering of graphene nanoribbons using strain.

In summary, our study shows that quantitative estimates of the electromechanical coupling in 2d materials – as is often required in strain-engineering applications – requires careful consideration of the lattice deformation on a microscopic level.

II. RESULTS

The atomic lattices of 2d materials are characterized by primitive unit cells (PUCs) with a set of basis atoms and two primitive lattice vectors $\mathbf{a}_1$ and $\mathbf{a}_2$. In a homogeneously strained sample it is sufficient to consider the deformation of a single unit cell under an applied strain. The deformed primitive lattice vectors read

$$\mathbf{a}_i' = (\mathfrak{I}_3 + \mathfrak{u}) \cdot \mathbf{a}_i, \tag{1}$$

where $\mathfrak{u}$ is the strain tensor and $i = 1, 2$. This equation also holds for nonuniform strain, for which $\mathfrak{u} = \mathfrak{u}(\mathbf{r})$ varies on length scales much longer than the lattice parameter. In general, the lattice vectors can be expressed by a linear combination of the bond vectors $\mathbf{r}_{jk}$,

$$\mathbf{a}_i = \sum_{\mathbf{r}_{jk} \in \{\mathbf{r}_c\}} C_{ijk} \mathbf{r}_{jk} \ , \tag{2}$$

where $\{\mathbf{r}_c\}$ is the set of bond vectors contained within each unit cell and C_{ijk} is a tensor encoding the lattice connectivity. We address the case where the strain field deforms the lattice, but preserves its connectivity. We show that for materials with a non-Bravais lattice structure, the modifications of the bond vectors due to strain

* croy@pks.mpg.de

do not follow Eq. (1). Let us start from the most general relation

$$\mathbf{r}'_{ij} = (\mathfrak{I}_3 + \mathfrak{u}) \cdot \mathbf{r}_{ij} + \mathbf{\Delta}_{ij} \ , \tag{3}$$

where the vectors $\mathbf{\Delta}_{ij}$ contain the differences between the strain displacement relations for $\mathbf{a}_i$ and $\mathbf{r}_{ij}$. The number of independent vectors $\mathbf{\Delta}_{ij}$ is determined by the number of basis atoms and $\sum_{\mathbf{r}_{jk}\in\{\mathbf{r}\}_c} C_{ijk}\mathbf{\Delta}_{jk} = 0$. For a Bravais lattice $\mathbf{\Delta}_{ij} = 0$. Each additional atom introduces three degrees of freedom, that can be expressed by an in-plane vector $\mathbf{\Delta}_\parallel$ and an out-of-plane component $\Delta_\perp\,\hat{z}$. The number of independent displacement vectors obtained in this way can, in general, be reduced by enforcing the lattice symmetry and connectivity. To be specific, we consider the most important 2d materials[11] under current investigation, divided in three groups, shown in Fig. S1.

The first class contains graphene and graphene-like materials, such as boron nitride, as well as non-planar materials, such as silicene and germanene. The PUC consists of two basis atoms and two lattice vectors $\mathbf{a}_1 = a_0\left(3/2, \sqrt{3}/2, 0\right)$ and $\mathbf{a}_2 = a_0\left(3/2, -\sqrt{3}/2, 0\right)$, see Fig. S1(a). The three nearest neighbor vectors are given by $\mathbf{r}_1 = (-a_0, 0, 0) - h\,\hat{z}$, $\mathbf{r}_2 = \mathbf{a}_1 + \mathbf{r}_1$ and $\mathbf{r}_3 = \mathbf{a}_2 + \mathbf{r}_1$, where h is the PUC corrugation height. The lattice vectors are written in terms of the bond vectors as $\mathbf{a}_1 = \mathbf{r}_2 - \mathbf{r}_1$ and $\mathbf{a}_2 = \mathbf{r}_3 - \mathbf{r}_1$. The bond vectors transform as $\mathbf{r}'_i = \mathbf{r}_i + \mathfrak{u}\cdot\mathbf{r}_i + \mathbf{\Delta}_i$, with the constraints $0 = \mathbf{\Delta}_2 - \mathbf{\Delta}_1$ and $0 = \mathbf{\Delta}_3 - \mathbf{\Delta}_1$. Hence, $\mathbf{\Delta}_i \equiv \mathbf{\Delta}$. The latter is conveniently expressed by in-plane deformations $\mathbf{\Delta}_\parallel$ and the corrugation change $\Delta_\perp\hat{z}$. Graphene is a special case for which $\Delta_\perp \equiv 0$.

The second class contains the transition metal dichalcogenides (TMDCs). Here the PUC contains three atoms, one transition metal (Mo or W) and two chalcogens (S or Se), see Fig. S1(b). The transition metal has six nearest neighbors. The bond vectors are labeled $\mathbf{r}_{1,u/d}$, $\mathbf{r}_{2,u/d}$ and $\mathbf{r}_{3,u/d}$ where the subscript u or d indicates whether the bond connects to the upper (u) or lower (d) layer of chalcogen atoms. The lattice vectors are given by $\mathbf{a}_1 = \mathbf{r}_{2,u/d} - \mathbf{r}_{1,u/d}$ and $\mathbf{a}_2 = \mathbf{r}_{3,u/d} - \mathbf{r}_{1,u/d1}$. The bond vectors transform as $\mathbf{r}'_{i,u/d} = \mathbf{r}_{i,u/d} + \mathfrak{u}\cdot\mathbf{r}_i + \mathbf{\Delta}_{i,\parallel} \pm \Delta_{i,\perp}/2\hat{z}$. The vectors $\mathbf{\Delta}_{i,\parallel}$ now satisfy $0 = \mathbf{\Delta}_{2,\parallel} - \mathbf{\Delta}_{1,\parallel}$ and $0 = \mathbf{\Delta}_{3,\parallel} - \mathbf{\Delta}_{1,\parallel}$. Consequently $\mathbf{\Delta}_{i,\parallel} \equiv \mathbf{\Delta}_\parallel$. By inversion symmetry, vectors connecting to the upper layer and the lower layer transform in the same way, but with opposite signs in the out-of-plane direction. Hence, the strain-displacement response of TMDCs is also characterized by a single in-plane vector $\mathbf{\Delta}_\parallel$ and the change in inter-chalcogen distance $\Delta_\perp$.

The third class consists of a single material, phosphorene, an atomically thin puckered material derived from layered black phosphorus. Its PUC contains four atoms and six unique bond vectors, see Fig. S1(c). Four bond vectors are situated in the puckers and are denoted by $\mathbf{r}_{i,u/d}$ with $i = 1,\ 2$ and subscripts u/d. The two remaining vectors connect the upper and lower puckers, and are labeled $\mathbf{r}_{cc}$ and $\mathbf{r}_{cc'}$. We find that $\mathbf{a}_1 = -\mathbf{r}_{cc} + \mathbf{r}_{1,u} + \mathbf{r}_{cc'} + \mathbf{r}_{2,d}$, and $\mathbf{a}_2 = -\mathbf{r}_{2,u} + \mathbf{r}_{1,u}$. Alternatively, we also write $\mathbf{a}_1 = -\mathbf{r}_{cc} + \mathbf{r}_{2,u} + \mathbf{r}'_{cc} + \mathbf{r}_{1,d}$ and $\mathbf{a}_2 = -\mathbf{r}_{2,d} + \mathbf{r}_{1,d}$. Hence, we obtain the constraints $0 = -\mathbf{\Delta}_{cc} + \mathbf{\Delta}_{1,u} + \mathbf{\Delta}_{cc'} + \mathbf{\Delta}_{2,d}$, $0 = -\mathbf{r}_{2,u} + \mathbf{r}_{1,u}$. This leads to four equations for the vectors $\mathbf{\Delta}_i$. Using inversion symmetry and the same arguments as for the TMDCs, the strain displacement relation in phosphorene is also characterized by a single in-plane vector $\mathbf{\Delta}_\parallel$ and a change in vertical inter-pucker distance $\Delta_\perp$.

We conclude that upon application of strain to all these 2d materials, due to lattice connectivity and symmetry constrains, the strain-displacement correction is simply

$$\mathbf{\Delta}_{ij} = \mathbf{\Delta}_\parallel + \Delta_\perp\hat{z}, \tag{4}$$

independent of i and j. Both $\mathbf{\Delta}_\parallel$ and $\Delta_\perp$ depend on the applied strain and on the interatomic interactions. Their calculation requires a microscopic model to account for the deformation energy. For uniform strain, one can determine the strain-displacement correction using the geometric considerations of the previous paragraph and, for instance, first principles calculations. For non-uniform strain and/or finite lattices, this procedure becomes computationally prohibitive, and one has to resort to semi-empirical force-field models.

In the following, we put forward a systematic and transparent approach to calculate $\mathbf{\Delta}_\parallel$ and $\Delta_\perp$ for any 2d material whose deformation energy is described by a force-field model parameterized by the bond vectors. Valence force models (VFMs) are a convenient choice since they offer good accuracy at low computational costs. There are various VFMs for the different 2d materials [12–16]. Let us focus on graphene-like materials, which can be accurately addressed using the VFM introduced by Perebeinos and Tersoff[14] to describe the interactions between sp^2-bonded carbon atoms. The deformation energy is given by[14]

$$\begin{aligned} E_{\rm def} = &\frac{\beta_r}{a_0^2}\sum_{i,j\in i}(\delta r_{ij})^2 + \beta_c\sum_{i,j<k\in i}(\delta c_{i,jk})^2 \\ &+ \frac{\beta_{r2}}{a_0^2}\sum_{i,j<k\in i}(\delta r_{ij})\,(\delta r_{ik}) \\ &+ \frac{\beta_{rc}}{a_0}\sum_{i,j\neq k<l\in i}(\delta r_{ij})\,(\delta c_{i,kl}) \\ &+ \frac{\beta_v}{a_0}\sum_{i,j<k<l\in i}\left(\frac{3\mathbf{r}'_{ij}\cdot\mathbf{r}'_{ik}\times\mathbf{r}'_{il}}{r_{ij}r_{ik} + r_{ik}r_{il} + r_{il}r_{ij}}\right)^2 , \end{aligned} \tag{5}$$

where $r_{ij} = |\mathbf{r}'_{ij}|$ is the bond length, $\delta r_{ij} = r'_{ij} - a_0$ is the change in bond length and $\delta c_{i,jk}$ is defined as $\delta c_{i,jk} = \cos\theta'_{i,jk} - \cos\theta_{i,jk}$. Here $\theta_{i,jk}$ is the angle between atoms i, j and k with atom i as apex in equilibrium, while $\theta'_{i,jk}$ is the angle in the deformed lattice. The summations in Eq. (5) follow the convention: (a) $j \in i$ indicates that the index j runs over the three neighbors of atom i; (b) for $j < k \in i$ both j and k are neighbors of the atom i, and are ordered to avoid double counting,

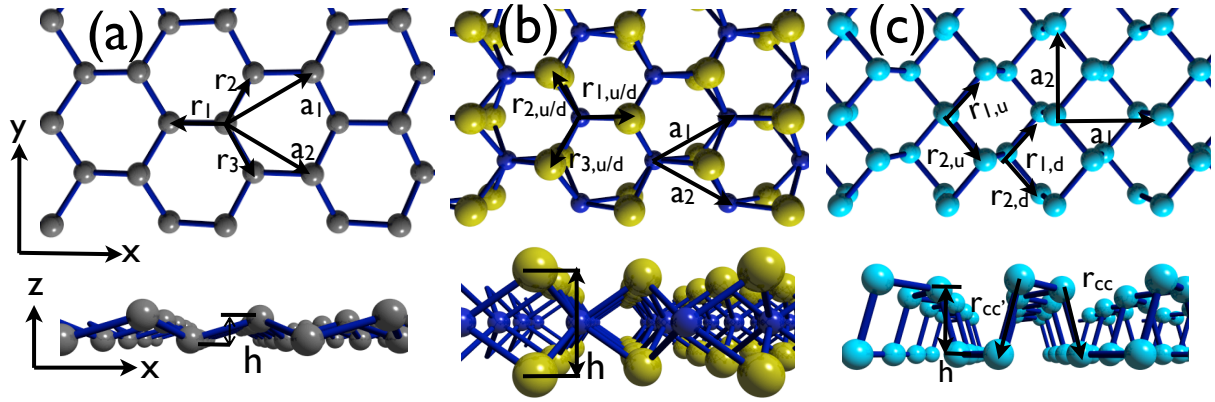

FIG. 1. Lattice structures of the three classes of 2d materials considered. a) The unit cell of graphene-like materials are defined by two lattice vectors $\mathbf{a}_1$ and $\mathbf{a}_2$ and three nearest neighbor vectors $\mathbf{r}_1$, $\mathbf{r}_2$ and $\mathbf{r}_3$. The material can in general be corrugated, signified by h in the lower figure. Graphene is contained as the case $h = 0$. b) The unit cell of TMDCs consist of two lattice vectors and three basis atoms, which define six nearest neighbor vectors. Due to the layered structure of the material, it has an effective thickness h. c) The phosphorene lattice is characterized by two lattice vectors and four basis atoms, defining ten nearest neighbor vectors. Its puckered structure gives rise to the effective thickness h.

leaving three possible terms; (c) $j \neq k < l \in i$ leaves three terms for each i. The first and second terms in Eq. (5) give the energy cost of stretching and bending bonds as in a Keating model[17]. The third and the fourth terms couple stretching of different bonds and couple stretching and bending, respectively. The last term is related to out-of-plane displacements. In Ref. 14, there is an additional term which penalizes misalignments of neighboring π-orbitals that we neglect here.

For a given strain, we minimize $E_{\rm def}$ with respect to $\mathbf{\Delta}_\parallel$ and $\Delta_\perp \hat{z}$ to obtain

$$\mathbf{\Delta}_\parallel \equiv -\frac{a_0\kappa(h)}{2}\begin{pmatrix} u_{yy}-u_{xx} \\ 2u_{xy} \\ 0 \end{pmatrix}, \tag{6a}$$

$$\Delta_\perp \equiv \pm a_0\kappa_\perp(h)(u_{xx}+u_{yy}), \tag{6b}$$

where $\kappa(h)$ and $\kappa_\perp(h)$ are functions of the unit cell corrugation height h and characterize the changes in the PUC internal structure, in addition to the trivial shift of atomic positions when the PUC is strained. To lowest order in h/a_0,

$$\kappa(h) \approx -\frac{9\beta_c - 4\beta_r + 2\beta_{r2}}{9\beta_c + 4\beta_r - 2(\beta_{r2}+3\beta_{rc})} \tag{7a}$$

$$\kappa_\perp(h) \approx -\frac{h}{a_0}\frac{2\beta_r + 2\beta_{r2} + 3\beta_{rc}}{9\beta_v}. \tag{7b}$$

Upon elimination of $\mathbf{\Delta}_\parallel$ and $\Delta_\perp$, the microscopic deformation energy per unit area, $\mathcal{E} = E_{\rm def}/\mathcal{A}$, becomes the standard expression for the continuum elastic energy-density of an isotropic membrane[4],

$$\begin{aligned}\mathcal{E} &= \frac{1}{2}\lambda(u_{xx}+u_{yy})^2 + \mu(u_{xx}^2+u_{yy}^2+2u_{xy}^2) \\ &= \frac{Y_{2d}}{2}(u_{xx}^2+u_{yy}^2+2\nu u_{xx}u_{yy}+(1-\nu)u_{xy}^2),\end{aligned} \tag{8}$$

reconciling our results with previous works on the long-wavelength elastic behavior of graphene[1, 19, 20]. Here, λ and μ are the Lamé parameters of the material, and Y_{2d} and ν are the $2d$ Young modulus and Poisson ratio, respectively. They are related via

$$Y_{\rm 2d} = \lambda + 2\mu, \quad \text{and} \quad \nu = \frac{\lambda}{\lambda+2\mu}. \tag{9}$$

We find that the Lamé parameters, given in terms of the microscopic parameters of Eq. (5), are

$$\begin{aligned}\lambda =& \frac{1}{\sqrt{3}a_0^2}\left[\frac{8\beta_r^2 - 18\beta_c\beta_r + 4\beta_r(\beta_{r2}-3\beta_{rc})}{9\beta_c+4\beta_r-2(\beta_{r2}+3\beta_{rc})}\right. \\ &\left.+\frac{9\beta_{rc}^2 - 36\beta_c\beta_{r2} - 4\beta_{r2}^2 - 12\beta_{rc}\beta_{r2}}{9\beta_c+4\beta_r-2(\beta_{r2}+3\beta_{rc})}\right],\end{aligned} \tag{10a}$$

$$\mu = \frac{3\sqrt{3}}{a_0^2}\left[\frac{4\beta_c\beta_r - 2\beta_c\beta_{r2} - \beta_{rc}^2}{9\beta_c+4\beta_r-2(\beta_{r2}+3\beta_{rc})}\right]. \tag{10b}$$

For graphene, the parameter values reported in Ref. 14 together with Eqs. (7) lead to $\kappa = 0.39$ and $\kappa_\perp = 0$. Moreover, Eqs. (10) give $\lambda = 4.4$ eV/Å^2 and $\mu = 8.8$ eV/Å^2, which implies $Y_{\rm 2d} = 352\,$N/m and $\nu = 0.2$.

Neglecting the bond-bond and bond-angle correlations in Eq. (5) (setting $\beta_{r2} = \beta_{rc} = 0$), we find that $\kappa(h)$ depends only on the Poisson ratio, $\kappa(h) \approx 2\nu/(1+\nu)$. Consequently, $\kappa(0)$ vanishes for materials with a negligible Poisson ratio (where $\mu \gg \lambda$), and is limited from above by $\kappa(0) < 2/3$ for isotropic materials (for which [4] $\nu < 1/2$). In this simplified VFM, $\kappa(0)$ agrees with the findings of Ref. 5, and may serve as a rough estimate, since it can be readily obtained form the Poisson ratio which is a macroscopically observable quantity. For $\nu = 0.2$ this approximation gives $\kappa \approx 1/3$, which agrees reasonably well with the value obtained from the full set of parameters ($\kappa = 0.39$). Similarly, we find $\kappa_\perp(h) \approx -2(h/a_0)(\beta_r/(9\beta_v))$.

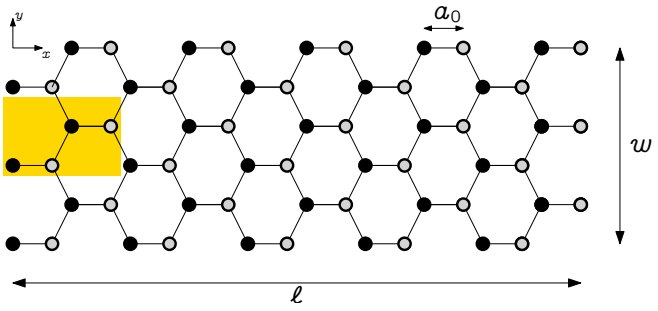

FIG. 2. Structure of an armchair nanoribbon. The highlighted area represents the system unit cell. The ribbon consists of $N_1 \times N_2$ cells, where N_1 counts the cells in x-direction and N_2 in y-direction. In the lateral direction periodic boundary conditions are imposed at the edges.

The approximation $\kappa \approx 2\nu/(1+\nu)$ is expected to hold also for TMDCs, due to the hexagonal structure of the lattice when projected onto the monolayer plane. For example, using $\nu_{MoS_2} = 0.27$ [21], we obtain $\kappa_{MoS_2} \approx 0.43$, which is slightly larger than the estimate for graphene. For phosphorene, the strain-displacement relation no longer obeys the simple form of Eq. (6), since $\mathbf{\Delta}$ shows a directionality reflecting the material anisotropy. Nonetheless, we can still use our theory to estimate the elastic properties of phosphorene (see Supplementary Material). Using a VFM developed for layered black phosphorus [2], we obtain sound velocities $v_{xx} = 3508$ m/s, $v_{yy} = 8147$ m/s, and $v_{xy} = 3707$ m/s in good agreement with Ref. 2 (without correction v_{xx} and v_{xy} are overestimated by a factor 2). The Young moduli are $Y_x = 17$ N/m and $Y_y = 94$ N/m (without corrections $Y_x = 58$ N/m and $Y_y = 95$ N/m). These values are in good agreement with DFT calculations [3, 5, 6], where $Y_x = 24 \ldots 29$ N/m and $Y_y = 88 \ldots 102$ N/m. Hence, a correct treatment of the strain-displacement relations is necessary to account for the predicted anisotropy of phosphorene[26].

We illustrate our results by studying armchair graphene nanoribbons (AGNRs) stretched along the longitudinal direction. See Fig. 2 for a sketch of the setup. The equilibrium configuration is obtained by minimizing $E_{\rm def}$, Eq. (5). The mechanical energy density as a function of the applied strain u_{xx} is shown in Fig. 3(a). Numerical results are denoted by symbols, whereas full and dashed lines correspond to analytical results obtained from Eq. (8) for $\kappa = 0.39$ and $\kappa = 0$. By setting $\kappa = 0$, one obtains a slightly larger value of Y_{2d} such that the stretching energy is overestimated. We also calculate the resulting strain u_{yy} in the transversal direction. As the ribbon contracts upon stretching, u_{yy} is negative for $u_{xx} > 0$ and decreases with increasing strain. This is shown in Fig. 3(b). The slope of the curve at $u_{xx} = 0$ gives the Poisson ratio, which agrees very well with the estimate obtained from Eq. (9). The standard approach, for which $\kappa = 0$, gives $\nu(\kappa = 0) \approx 0.16$, thus underestimating the Poisson ratio.

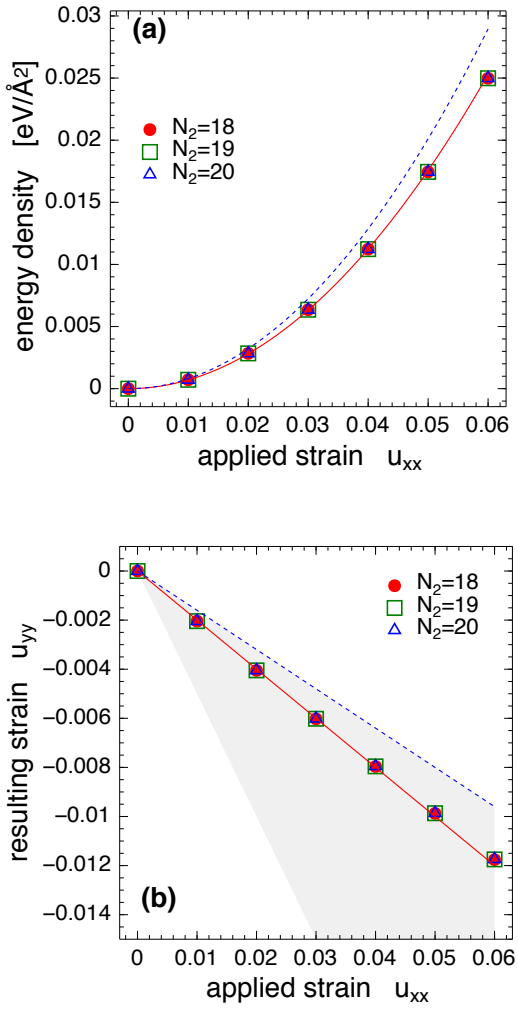

FIG. 3. Strain u_{xx} dependence of (a) the elastic energy and (b) the resulting strain u_{yy} for AGNRs of different widths ($N_1 = 300$ in all cases). Symbols denote numerical results. The full (dashed) line stands for the continuum model results with $\kappa \approx 0.39$ ($\kappa = 0$). The shaded region indicates the range of Poisson ratios from $\nu(\kappa = 0) = 0.16$ to $\nu = 1/2$.

The strain-displacement relations presented above significantly modify the electronic properties of deformed 2d materials, which are crucial for strain-engineering[3, 4, 27]. Essentially, mechanical deformations have two effects on the electrons. Firstly, the change in electron-ion potential in the neighborhood of an atom generates an on-site potential often referred to as the deformation potential. Secondly, changes in the distances between neighboring atoms modify the overlaps of the corresponding orbital wave-functions and thus the electronic structure.

These effects are accounted for in the nearest-neighbor hopping Hamiltonian which provides an accurate description of the low-energy π-bands in graphene[2, 5, 7],

namely,

$$H = \sum_{i=1}^{N_{\rm at}} \left[\left(3v_0(a_0) + \frac{g}{a_0} \sum_{<k,i>} \frac{\mathbf{r}_{ik} \cdot \delta\mathbf{r}_{ik}}{a_0} \right) c_i^\dagger c_i \right. \\ \left. - t_0(a_0) \sum_{<j,i>} \left(1 - \frac{\beta}{a_0} \frac{\mathbf{r}_{ij} \cdot \delta\mathbf{r}_{ij}}{a_0} \right) c_i^\dagger c_j \right] . \quad (11)$$

Here $\beta/a_0 = -t_0'(a_0)/t_0(a_0)$, $g/a_0 = v_0'(a_0)$, where $t_0(r)$ is the (distance dependent) hopping amplitude and $v_0(r)$ is the electron-ion potential. In the following we omit the overall on-site energy $3v_0(a_0)$.

To obtain analytical insight, it is customary [2, 7–9] to consider the low-energy limit of the tight-binding model above. By expressing Eq. (11) in reciprocal space and taking its long wavelength limit, that is, by expanding H to linear order in momentum around the $\mathbf{K}$ and $\mathbf{K}'$-points [2, 7], one obtains an effective Dirac Hamiltonian. For $\mathbf{K}$ we write

$$H_{\mathbf{K}} = v_F \boldsymbol{\sigma} \cdot (\mathbf{p} - \mathbf{A}) + v_{\rm D} \mathfrak{I}_2 \, , \quad (12)$$

where $v_F = 3a_0 t_0/2 \approx 10^5$ m/s, $\boldsymbol{\sigma}$ are Pauli matrices, $\mathbf{p}$ is the momentum, $\mathbf{A}$ is the vector potential, and $v_{\rm D}$ is the scalar deformation potential. The latter are given by

$$A_x = \frac{\beta(1-\kappa)}{a_0} u_{xy} \quad (13a)$$

$$A_y = \frac{\beta(1-\kappa)}{2a_0} \left(u_{yy} - u_{xx} \right) \, , \quad (13b)$$

$$v_{\rm D} = \frac{3g}{2} \left[1 + 2\kappa_\perp(h) h \right] \left(u_{xx} + u_{yy} \right) \, . \quad (13c)$$

Hence, we find that the strain-displacement relations renormalize $\mathbf{A}$ by a factor $1-\kappa$ with respect to the standard elasticity-induced gauge theory [7, 8, 28–31]. For graphene, the material parameters[14] give $1-\kappa \approx 3/5$. (Using the approximation $\kappa \approx 2\nu/(1+\nu)$ we obtain $1-\kappa \approx (1-\nu)/(1+\nu) = 2/3$.) Based on a VFM that drastically overestimates the Poisson ratio, previous works[5, 10] report a reduction factor of about 1/3. Note that in the derivation above, we ignore the strain-dependent renormalization of the Fermi velocity reported previously[31], since it has a negligible effect on our results.

The reduced vector potential has an important effect on strain engineering applications[28, 30]. Let us analyze, for instance, the first (sub)band-gap of AGNRs[27]. In the long wavelength limit, the magnitude of this band gap is given by

$$E_g \approx \sqrt{3}|t_0| \min_{n=0,1,\ldots} \left| \frac{\pi}{N_2+1}(n-\phi) \right. \\ \left. - \frac{\sqrt{3}\beta_D}{2}(1-\kappa)(1+\nu) u_{xx} \right| \quad (14)$$

with $\phi = 0$ for metallic and $\phi = 1/3$ for semiconducting AGNRs and where N_2 is the number of unit cells in the transversal direction and n is the band index. The magnitude of the band-gap as a function of strain is piecewise linear and shows a characteristic zig-zag shape. We predict that the slope of the linear regions is decreased by a factor $(1-\kappa)(\approx 3/5$ for graphene) due to the strain-displacement relations, while the positions of the maxima and minima of the band gap are shifted by a factor $1/(1-\kappa)(\approx 5/3$ for graphene).

We verify this prediction numerically. First, we obtain the relaxed lattice structure of a stretched AGNR as described previously. Subsequently, we diagonalize the Hamiltonian (11) using $t_0 = 2.8$ eV, $g = 4$ eV, $\beta = 3.37$[2, 3], and the relaxed lattice structure as an input. From the eigenvalues we directly calculate the band-gap $E_{\rm g}$ shown in Fig. 4. For comparison we also show $E_{\rm g}$ for $\kappa = 0$. For the considered range of applied strain we find a good agreement between the numerical results and Eq. (14). We observed that the strain required to achieve a certain gap size increases for $\kappa > 0$.

A similar renormalization is also found for phosphorene. Based on the two orbital tight-binding model put forward in Ref. 7 and the strain-displacement relations derived in the supplementary material we find an *anisotropic* renormalization of the strain-induced band-gap. It is reduced by factors 2.5 and 1.35 when straining in x and y direction, respectively.

III. CONCLUSIONS

Two-dimensional materials have gained considerable interest, in particular due to the enticing prospect of engineering their electronic properties using strain. Our results show that the relationship between strain and electronic properties is less trivial than often assumed. For Bravais lattices, the relation between strain and displacements is simple, namely the bond vectors transform as $\mathbf{r}_{ij} \to (\mathfrak{I}_3 + \mathfrak{u}) \cdot \mathbf{r}_{ij}$. For non-Bravais lattices, the basis atoms introduce additional degrees of freedom, significantly modifying the relation between strain and displacement. With few exceptions[5, 10], this fact is typically neglected in the literature on electronic properties of deformed 2d materials [3, 4, 6, 7, 28–30]. We show that under an applied strain the bond vectors of 2d materials generally transform as $\mathbf{r}_{ij} \to (\mathfrak{I}_3 + \mathfrak{u}) \cdot \mathbf{r}_{ij} + \boldsymbol{\Delta}_\parallel + \Delta_\perp \hat{z}$. The vectors $\boldsymbol{\Delta}_\parallel$ and $\Delta_\perp \hat{z}$ are determined by minimizing the deformation energy. For graphene, the strain-displacement effect on the electronic properties is to renormalize the vector potential by a factor $(1-\kappa) \approx 3/5$ while keeping its functional form. We provide a simple estimate of this correction based on the macroscopically observable Poisson ratio ν, as $(1-\kappa) \approx (1-\nu)/(1+\nu)$. The $(1-\kappa)$ renormalization alters the dependence of the band gap in AGNRs on strain: it increases the strain required to reach a certain band gap. Having a well

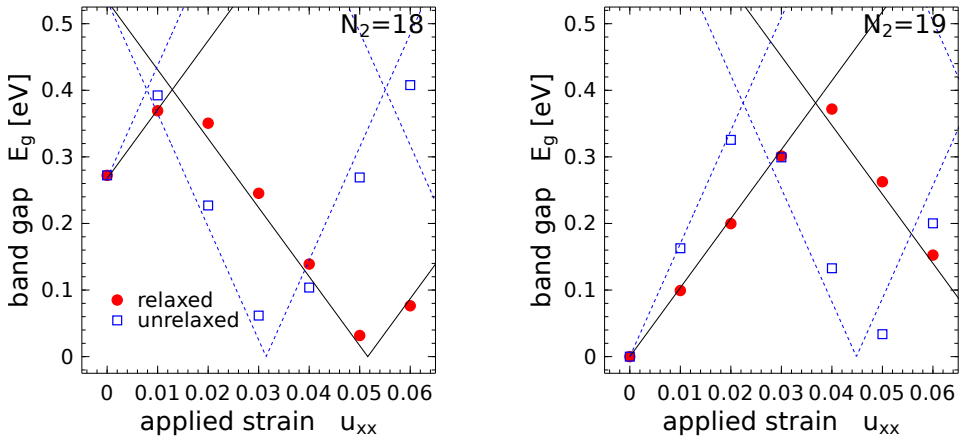

FIG. 4. Strain dependence of the (first) gap size for AGNRs of different widths ($N_1 = 300$ in all cases). Symbols represent tight-binding calculations without (blue) and with relaxation (red). The dashed (solid) lines show the effective Dirac equation, Eq. (14), results for $\kappa = 0$ ($\kappa \approx 0.39$).

controlled band gap is of key importance in a variety of applications[3, 4, 33–35].

For 2d materials with a more complex crystal structure than graphene, such as the TMDCs and phosphorene, the strain-displacement relations we put forward are key to understand their fundamental material properties. For phosphorene, we show (see Supplementary Material) that its anisotropic mechanical properties[3, 36] can only be obtained by considering proper strain-displacement relations. Furthermore, phosphorene is considered to be very interesting from a strain-engineering perspective as it displays a strain dependent band-gap[37–39]. Our strain-displacement relations lead to an anisotropic renormalization of this gap. This Letter provides a transparent approach to estimate the electromechanical coupling in 2d materials, given that the mechanical and electrical properties are reliably parameterized.

ACKNOWLEDGMENTS

The authors thank Andreas Isacsson and Nuno Peres for helpful comments.

[1] Atalaya, J.; Isacsson, A.; Kinaret, J. M. *Nano Lett.* **2008**, *8*, 4196–4200.
[2] Castro Neto, A. H.; Guinea, F.; Peres, N. M. R.; Novoselov, K. S.; Geim, A. K. *Rev. Mod. Phys.* **2009**, *81*, 109–162.
[3] Pereira, V. M.; Castro Neto, A. H.; Peres, N. M. R. *Phys. Rev. B* **2009**, *80*, 045401.
[4] Pereira, V. M.; Castro Neto, A. H. *Phys. Rev. Lett.* **2009**, *103*, 046801.
[5] Suzuura, H.; Ando, T. *Phys. Rev. B* **2002**, *65*, 235412.
[6] Mañes, J. L. *Phys. Rev. B* **2007**, *76*, 45430.
[7] Vozmediano, M. A. H.; Katsnelson, M. I.; Guinea, F. *Phys. Rep.* **2010**, *496*, 109.
[8] Couto, N. J. G.; Costanzo, D.; Engels, S.; Ki, D.-K.; Watanabe, K.; Taniguchi, T.; Stampfer, C.; Guinea, F.; Morpurgo, A. F. *Phys. Rev. X* **2014**, *4*, 041019.
[9] Burgos, R.; Warnes, J.; Lima, L. R. F.; Lewenkopf, C. *Phys. Rev. B* **2015**, *91*, 115403.
[10] Woods, L. M.; Mahan, G. D. *Phys. Rev. B* **2000**, *61*, 10651–10663.
[11] Miro, P.; Audiffred, M.; Heine, T. *Chem. Soc. Rev.* **2014**, *43*, 6537–6554.
[12] Kaneta, C.; Katayama-Yoshida, H.; Morita, A. *J. Phys. Soc. Jpn.* **1986**, *55*, 1213–1223.
[13] Wakabayashi, N.; Smith, H. G.; Nicklow, R. M. *Phys. Rev. B* **1975**, *12*, 659–663.
[14] Perebeinos, V.; Tersoff, J. *Phys. Rev. B* **2009**, *79*, 241409.
[15] Jiang, J.-W.; Park, H. S.; Rabczuk, T. *Journal of Applied Physics* **2013**, *114*, 064307.
[16] Jiang, J.-W. arXiv:1504.02847.
[17] Keating, P. N. *Phys. Rev.* **1966**, *145*, 637–645.
[4] Landau, L. D.; Lifshitz, E. M. In *Theory of elasticity*, 3rd ed.; Kosevich, A. M., Pitaevski\u\i, L. P., Eds.; Butterworth-Heinemann: Oxford, 1986.
[19] Lee, C.; Wei, X.; Kysar, J. W.; Hone, J. *Science* **2008**, *321*, 385–388.
[20] Zhang, D.-B.; Akatyeva, E.; Dumitrica, T. *Phys. Rev. Lett.* **2011**, *106*.
[21] Feldman, J. L. *J. Phys. Chem. Solids* **1976**, *37*, 1141–1144.
[2] Kaneta, C.; Katayama-Yoshida, H.; Morita, A. *Solid State Communications* **1982**, *44*, 613–617.
[3] Wei, Q.; Peng, X. *Appl. Phys. Lett.* **2014**, *104*, 251915.
[6] Qiao, J.; Kong, X.; Hu, Z.-X.; Yang, F.; Ji, W. *Nat Commun* **2014**, *5*, 4475.
[5] Elahi, M.; Khaliji, K.; Tabatabaei, S. M.; Pourfath, M.; Asgari, R. *Phys. Rev. B* **2015**, *91*, 115412.

[26] Jiang, J.-W.; Park, H. S. *Nat Commun* **2014**, *5*, 4727.
[27] Lu, Y.; Guo, J. *Nano Research* **2010**, *3*, 189–199.
[28] Guinea, F.; Katsnelson, M. I.; Geim, A. K. *Nat Phys* **2010**, *6*, 30–33.
[29] Levy, N.; Burke, S. A.; Meaker, K. L.; Panlasigui, M.; Zettl, A.; Guinea, F.; Castro Neto, A. H.; Crommie, M. F. *Science* **2010**, *329*, 544.
[30] Low, T.; Guinea, F.; Katsnelson, M. I. *Phys. Rev. B* **2011**, *83*, 195436.
[31] de Juan, F.; Sturla, M.; Vozmediano, M. A. H. *Phys. Rev. Lett.* **2012**, *108*, 227205.
[7] Jiang, J.-W.; Park, H. S. *Phys. Rev. B* **2015**, *91*, 235118.
[33] Castellanos-Gomez, A.; Roldán, R.; Cappelluti, E.; Buscema, M.; Guinea, F.; van der Zant, H. S. J.; Steele, G. A. *Nano Letters* **2013**, *13*, 5361–5366.
[34] Yang, L.; Cui, X.; Zhang, J.; Wang, K.; Shen, M.; Zeng, S.; Dayeh, S. A.; Feng, L.; Xiang, B. *Sci. Rep.* **2014**, *4*.
[35] Midtvedt, D.; Croy, A. arXiv:1504.06956.
[36] Jiang, J.-W.; Rabczuk, T.; Park, H. *Nanoscale* **2015**, *7*, 6059.
[37] Han, X.; Morgan Stewart, H.; Shevlin, S. A.; Catlow, C. R. A.; Guo, Z. X. *Nano Lett.* **2014**, *14*, 4607–4614.
[38] Peng, X.; Wei, Q.; Copple, A. *Phys. Rev. B* **2014**, *90*, 85402.
[39] Fei, R.; Yang, L. *Nano Lett.* **2014**, *14*, 2884–2889.

Supplemental Materials: Strain-displacement relations and strain engineering in 2d materials

STRAIN-DISPLACEMENT RELATIONS FOR BLACK PHOSPHOROUS

Black phosphorous is a two-dimensional material with an orthorhombic lattice-structure with lattice vectors $\mathbf{a}_1$ and $\mathbf{a}_2$, and four basis atoms arranged in a puckered structure (see Fig. S1). The bond vectors have approximately equal length $d \approx 2.24$ Å, and intra- and inter-pucker angles $\Theta_1 = \Theta_{328} \approx 96.3^{\text{o}}$ and $\Theta_2 = \Theta_{123} \approx 102^{\text{o}}$ [S1]. Hence, the bond vectors read

$$\mathbf{r}_{12} = [-d\cos(\Theta_2)/\cos(\Theta_1/2), 0, d\sqrt{1-(\cos(\Theta_2)/\cos(\Theta_1/2))^2}] \,, \tag{S1a}$$

$$\mathbf{r}_{23} = [d\cos(\Theta_1/2), d\sin(\Theta_1/2), 0] \,, \tag{S1b}$$

$$\mathbf{r}_{43} = [d\cos(\Theta_1/2), -d\sin(\Theta_1/2), 0] \,. \tag{S1c}$$

with $\mathbf{r}_{43} = \mathbf{r}_{28} = \mathbf{r}_{61}$, $\mathbf{r}_{23} = \mathbf{r}_{41} = \mathbf{r}_{71}$, $\mathbf{r}_{12} = \mathbf{r}_{54}$ and $\mathbf{r}_{39} = [r_{12,x}, r_{12,y}, -r_{12,z}]$. A lattice deformation, cast in terms of the strain tensor $\mathfrak{u}$, modifies the bond vectors as

$$\mathbf{r}'_{12} = \mathbf{r}_{12} + \mathfrak{u}\cdot\mathbf{r}_{12} + \boldsymbol{\Delta}_{\parallel} + \boldsymbol{\Delta}_{\perp}\hat{z} \,, \tag{S2a}$$

$$\mathbf{r}'_{23} = \mathbf{r}_{23} + \mathfrak{u}\cdot\mathbf{r}_{23} - \boldsymbol{\Delta}_{\parallel} \,, \tag{S2b}$$

$$\mathbf{r}'_{43} = \mathbf{r}_{43} + \mathfrak{u}\cdot\mathbf{r}_{43} - \boldsymbol{\Delta}_{\parallel} \,. \tag{S2c}$$

We assume that $\mathbf{r}'_{43} = \mathbf{r}'_{28} = \mathbf{r}'_{61}$, $\mathbf{r}'_{23} = \mathbf{r}'_{41} = \mathbf{r}'_{71}$, $\mathbf{r}'_{12} = \mathbf{r}'_{54}$ and $\mathbf{r}'_{39} = [r'_{12,x}, r'_{12,y}, -r'_{12,z}]$.

According to the VFM put forward in Ref. S2 (see also Ref. S1) the elastic energy of the unit cell is given by

$$\begin{aligned} E_{\text{cell}} = {} & K_r d^2\,(\delta r_{23})^2 + K_r d^2\,(\delta r_{28})^2 + K'_r d^2\,(\delta r_{21})^2 \\ & + 2K_\Theta d^2\,(\delta\Theta_{328})^2 + 2K'_\Theta d^2\,(\delta\Theta_{321})^2 + 2K'_\Theta d^2\,(\delta\Theta_{821})^2 \\ & + 2K_{rr'} d^2\,(\delta r_{23}\delta r_{28}) + 2K'_{rr'} d^2\,(\delta r_{23}\delta r_{21}) + 2K'_{rr'} d^2\,(\delta r_{28}\delta r_{21}) \\ & + 2K_{r\Theta} d^2\,(\delta r_{23}\delta\Theta_{234}) + 2K_{r\Theta} d^2\,(\delta r_{43}\delta\Theta_{234}) + 2K'_{r\Theta} d^2\,(\delta r_{23}\delta\Theta_{123}) + 2K'_{r\Theta} d^2\,(\delta r_{28}\delta\Theta_{128}) \\ & + 2K''_{r\Theta} d^2\,(\delta r_{12}\delta\Theta_{123}) + 2K''_{r\Theta} d^2\,(\delta r_{12}\delta\Theta_{128}) \,, \end{aligned} \tag{S3}$$

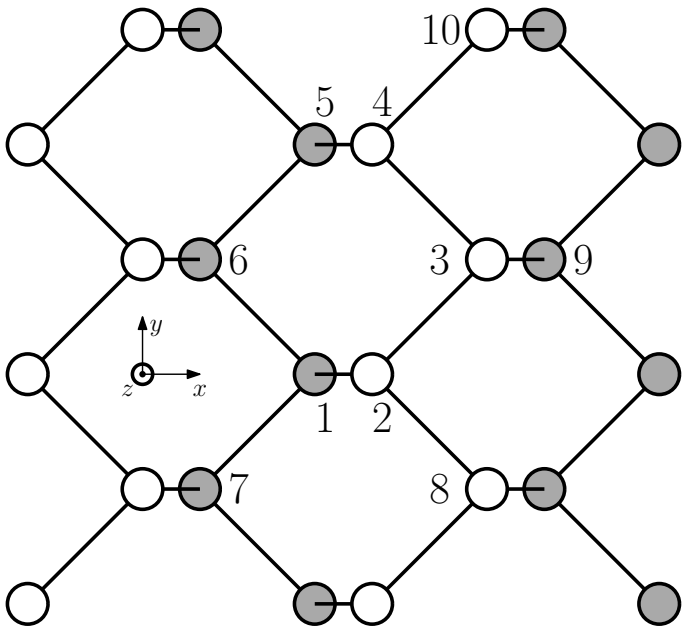

FIG. S1. Lattice structures of phosphorene. It is characterized by two lattice vectors and four basis atoms $(1, 2, 3, 4)$, defining ten nearest neighbor vectors.

	Y_x	Y_y	G_{xy}
without correction	58	95	51
with correction	17	94	20
	v_{xx}	v_{yy}	v_{xy}
without correction	6993	8930	5957
with correction	3508	8147	3707
Kaneta et al. [S2]	3720	8190	3760

TABLE S1. Young's and shear moduli and sound velocities from Eqs. (S6) and (S7). The former are given in units of N/m and the latter in m/s.

where $\delta r_{ij} = |\mathbf{r}'_{ij} - \mathbf{r}_{ij}|/d \approx (\mathbf{r}'_{ij} - \mathbf{r}_{ij}) \cdot \mathbf{r}_{ij}/d^2$ is the relative bond-length change and $\delta\Theta_{ijk} \approx -(\cos(\Theta'_{ijk}) - \cos(\Theta_{ijk}))/\sin(\Theta_{ijk})$ with $\cos(\Theta'_{ijk}) \approx (\mathbf{r}'_{ij}\cdot\mathbf{r}'_{jk})(1-\delta r_{ij}/d-\delta r_{jk}/d)/d^2$ is the bond angle change due to the deformation up to first order in strain and $\mathbf{\Delta}$. There are nine force-field parameters, namely, K_r, K'_r, K_Θ, K'_Θ, $K_{rr'}$, $K_{r\Theta}$, $K'_{r\Theta}$ and $K''_{r\Theta}$. Those determine the energy cost for bond stretching, angle bending, bond-bond and bond-angle correlations. The expressions for the bond vectors, Eqs. (S1) and (S2), render the energy $E_{\rm cell}$, Eq. (S3), to be a quadratic function in the components of the strain tensor and the components of $\mathbf{\Delta}$. By minimizing $E_{\rm cell}$ with respect to $\Delta_{\parallel,x}$, $\Delta_{\parallel,y}$ and $\Delta_\perp$ and dividing by the area of the unit cell, $A_{\rm cell}$, we obtain the deformation energy-density $\mathcal{E}_{\rm cell} = E_{\rm cell}/A_{\rm cell}$. For the VFM parameters reported in Ref. S2 we find

$$\Delta_{\parallel,x} = 0.61d\ u_{xx} + 0.37d\ u_{yy}\ , \quad \Delta_{\parallel,y} = 1.02d\ u_{xy}\ , \quad \Delta_\perp = -0.36d\ u_{xx} - 0.20d\ u_{yy}\ . \tag{S4}$$

These expressions, together with Eqs. (S2), constitute the strain-displacement relations for phosphorene.

A. Elasticity constants

Having the deformation energy-density $\mathcal{E}_{\rm cell}$ one can calculate the elastic constants C_{ij}, which are given by[S3]

$$C_{ij} = \frac{\partial^2 \mathcal{E}_{\rm cell}}{\partial u_i \partial u_j}\ , \tag{S5}$$

where $i,j = 1,2,6$ and $u_1 = u_{xx}$, $u_2 = u_{xx}$ and $u_6 = u_{xy}$. From those one derives Young's and shear moduli, $Y_{x/y}$ and G_{xy}, and the Poisson ratios $\nu_{xy/yx}$,

$$Y_x = \frac{C_{11}C_{22} - C_{12}^2}{C_{22}}\ , \quad Y_y = \frac{C_{11}C_{22} - C_{12}^2}{C_{11}}\ , \quad G_{xy} = C_{66}\ , \quad \nu_{xy} = \frac{C_{12}}{C_{22}}\ , \quad \nu_{yx} = \frac{C_{12}}{C_{11}}\ . \tag{S6}$$

Moreover, the sound velocities are given by[S4]

$$v_{xx} = \sqrt{\frac{C_{11}}{\rho_P}}\ , \quad v_{xx} = \sqrt{\frac{C_{22}}{\rho_P}}\ , \quad v_{xy} = \sqrt{\frac{C_{66}}{\rho_P}}\ , \tag{S7}$$

where ρ_P is the 2d mass density of phosphorene.

The results we calculate for all those elastic properties are summarized in Tab. S1. We also provide results for the case where the correction $\mathbf{\Delta}$ is not taken into account. Comparing the sound velocities to the values given in Ref. S2 one readily concludes that is necessary to account for $\mathbf{\Delta}$ to get comparable results. One may also compare the Young's moduli to recent DFT results from various groups. There the values of the reported Young's moduli are for instance: 26 N/m and 88 N/m [S5], 24 N/m and 92 N/m [S3], 29 N/m and 102 N/m [S6]. Again the values in Tab. S1 for the corrected case match best.

Qualitatively, the VFM reported in Ref. S2 gives very good results. However, it should also be mentioned that it has some deficits. For example, the Poisson ratios are obtained as $\nu_{yx} = 0.27$ and $\nu_{xy} = 0.05$, whereas other studies report 0.81/0.24[S5] or 0.62/0.17[S3]. However, it should be kept in mind that the parameters of the VFM were found by fitting to optical Γ-phonons measured in an experiment. To get a better quantitative description more data is required and the Poisson ratios need to be included in the fitting procedure.

B. Electronic band-gap

As argued in the main text, the strain-displacement relations are very important for correctly estimating the influence of strain on the electronic structure. To demonstrate this for phosphorene, we follow Ref. S7 where a two-orbital tight-binding model was used to calculate the electronic band-gap of phosphorene. The band-gap energy is then given by

$$E_{\mathrm{gap}} = 2(t_1 + t_2 + t_3) \,, \tag{S8}$$

where t_1, t_2 and t_3 are the hopping parameters between atoms 2 and 3, 2 and 1 and 2 and 8, respectively. For the undeformed lattice the values are $t_1^0 = t_3^0 = -0.797$ eV and $t_2^0 = 2.393$ eV. Assuming a distance dependence of the hopping parameters as $t(r) \propto 1/r^2$, in accordance with the nature of the orbitals responsible for the relevant electronic bands, allows it to calculate the strain-induced modification of the band-gap ΔE_{gap}. To this end we use the strain-displacement relations, Eq. (S2) and (S4), for the respective bond-lengths. We obtain

$$\text{without correction:} \qquad \Delta E_{\mathrm{gap}} \approx 1.899 u_{xx} + 3.538 u_{yy} \,, \tag{S9}$$

$$\text{with correction:} \qquad \Delta E_{\mathrm{gap}} \approx 0.755 u_{xx} + 2.612 u_{yy} \,. \tag{S10}$$

For comparison, in Ref. S7 the band-gap modification $\Delta E_{\mathrm{gap}} \approx 1.863 u_{xx} + 3.507 u_{yy}$ was obtained by transforming all bond-vectors using the strain tensor only. Similar to the case of graphene, one obtains a non-negligible renormalization due to the non-Bravais nature of the lattice.

[S1] Jiang, J.-W. arXiv:1503.00200.
[S2] Kaneta, C.; Katayama-Yoshida, H.; Morita, A. *Solid State Communications* **1982**, *44*, 613–617.
[S3] Wei, Q.; Peng, X. *Appl. Phys. Lett.* **2014**, *104*, 251915.
[S4] Landau, L. D.; Lifshitz, E. M. In *Theory of elasticity*, 3rd ed.; Kosevich, A. M., Pitaevski\u\i, L. P., Eds.; Butterworth-Heinemann: Oxford, 1986.
[S5] Elahi, M.; Khaliji, K.; Tabatabaei, S. M.; Pourfath, M.; Asgari, R. *Phys. Rev. B* **2015**, *91*, 115412.
[S6] Qiao, J.; Kong, X.; Hu, Z.-X.; Yang, F.; Ji, W. *Nat Commun* **2014**, *5*, 4475.
[S7] Jiang, J.-W.; Park, H. S. *Phys. Rev. B* **2015**, *91*, 235118.